34th Annual International Conference of the IEEE EMBS
San Diego, California USA, 28 August - 1 September, 2012

In Vitro Study of Iridium Electrodes for Neural Stimulation

Naser Pour Aryan[1], Christian Brendler[1], Viola Rieger[1], Sebastian Schleehauf[2], Gerhard Heusel[3], and Albrecht Rothermel[1]

***Abstract*— Iridium is one of the main electrode materials for applications like neural stimulation. Iridium has a higher charge injection capacity when activated and transformed into AIROF (activated iridium oxide film) using specific electrical signals [1]. Activation is not possible in stimulating devices, if they do not include the necessary circuitry for activation. We introduce a method for iridium electrode activation requiring minimum additional on-chip hardware. In the main part, the lifetime behavior of iridium electrodes is investigated. These results may be interesting for applications not including on-chip activation hardware, and also because activation has drawbacks such as worse mechanical properties and reproducibility of AIROF.**

I. INTRODUCTION

LIFETIME and sustenance are crucial parameters for any neural stimulation device. Among the most determining factors for device stability is the electrode resistance to corrosion and break down caused by injecting charge into the ambient tissue environment. Electrode material resistance to this corrosion can be explained in terms of charge injection capacity [2][3][4][5]. Our previous study showed that iridium has already a higher charge injection capacity compared to TiN [1]. Activation using a cyclically varying voltage between -0.7V and +1.2V enhances the charge injection capacity within the water window considerably [1] (Method from [12]).

Activating iridium has some drawbacks. Activated iridium (AIROF) has reduced mechanical properties compared to iridium. It is also worse regarding susceptibility to process variations (reproducibility) [6].

In this paper, we suggest an additional switch to ground for each electrode to activate electrodes on a neural stimulation chip. In the next part, we present our results regarding iridium electrode lifetime in a quantitative manner (compared to our more qualitative approach in [2] regarding TiN).

We use microelectrode arrays (MEAs) to study the electrode behavior. The electrodes on these MEAs are directly accessible via gold lines. The electrodes may be accessed in 4-fold batches. Every electrode has a square area of 50μm x 50μm. The distance between the electrodes is 20μm. A picture of a part of a MEA containing 64 electrodes is shown in Fig. 1.

Throughout all experiments, the electrolyte was phosphate buffered saline (PBS). The counter electrode had a much larger area than the MEA electrodes (about 0.5cm^2). To avoid any galvanic effects, the counter electrode material was chosen to be iridium. We did not activate the counter electrode to avoid any additional electromotive force (emf), which could drive undesired reactions because of the half-cell potential difference between iridium (working electrode) and iridium oxide (counter electrode).

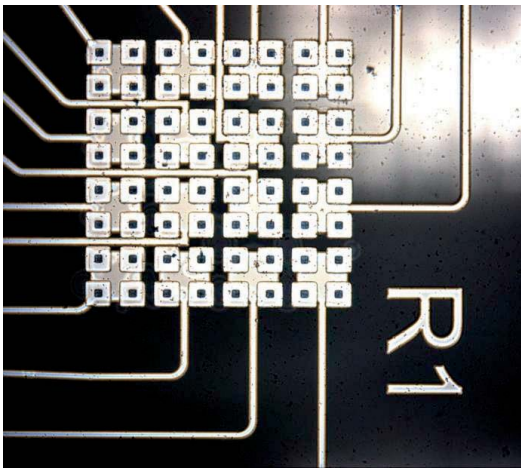

Fig. 1. Part of a MEA containing 64 electrodes. Every 4 electrodes are connected together.

II. FABRICATION PROCESS OF MICRO ELECTRODE ARRAYS (MEAS)

The MEAs are manufactured using thin film lithography on a float glass substrate. Gold lines are patterned with a lift-off technique on the surface of the substrate. The metal lines are covered with a polyimide insulation layer. A hard mask is used to remove the polyimide at the electrode sites and over the conduction pads. The iridium electrodes are patterned in a subsequent lift-off process. The profile of one electrode is shown in Fig 2.

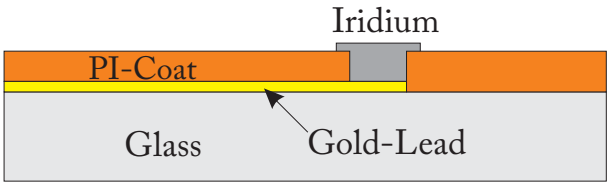

Fig. 2. Profile of MEA [1]

[1]Institute of Microelectronics, University of Ulm, Ulm, 89081, Germany
[2]Retina Implant AG, Reutlingen, 72770, Germany
[3]Natural and Medical Sciences Institute at University of Tuebingen, Reutlingen, 72770, Germany

III. IRIDIUM ACTIVATION

Activating iridium requires a ramp voltage, cyclically varying between -0.7V and +1.2V with 100mV/s rate for 500 cycles [1]. Neural stimulation chips may not provide a capability for the electrode output to have such a signal. Stimulator chips like [8],[9], &[10] are designed to deliver biphasic symmetrical current pulses in order to ensure charge balance at the output. Generation of electrode activation waveform is not reported.

In order to support activation, we suggest a switch to connect the electrodes to the system ground. Now the electrodes can be activated by cyclically varying the counter electrode voltage with a waveform reversed to the one mentioned above, i.e. cyclically varied between -1.2V and +0.7V.

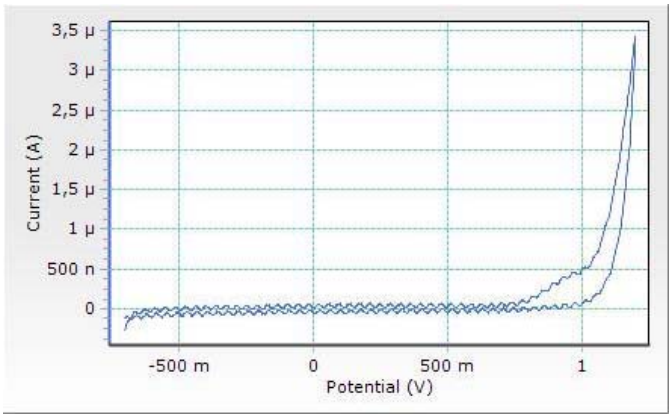

Fig. 3. Cyclic voltammetry curve corresponding to the cycle having maximum current over the voltage among the 500 activation cycles. This curve usually occurs at the beginning.

The cyclic voltammetry diagram of the cycle in the activation pulse train (composed of 500 ramp pulses explained above), having the highest current for the peak positive and negative electrode voltages is shown in Fig. 3. This diagram was measured by connecting a VersaSTAT 4 potentiostat to one of the 4-fold electrode batches. This cycle is usually in the beginning among the 500 pulses. The next pulses pull less current out of the electrode, i.e. the electrode current versus electrode voltage cyclic voltammetry curve decreases in amplitude as activation proceeds. From Fig. 3, we see that the activation current for 4 electrodes has a maximum of 3.5μA, corresponding to a maximum activation current per electrode of about 0.87μA. Such a current can be provided by an NMOS or PMOS transistor switch having small area without significant voltage drop.

IV. IRIDIUM LIFETIME ANALYSIS

Iridium has better mechanical properties and a higher degree of reproducibility compared to AIROF. This was our motivation to study the lifetime of iridium electrodes depending on the charge injection amplitude.

For our experiments, a test arrangement was designed including a laptop, an NI-6259 multifunctional board, electrode driving circuitry and several MEAs. The whole system is controlled by a LabVIEW computer program. A pulse voltage source provides biphasic voltage signals with 0.3ms cathodic pulse length, 0.5ms anodic pulse length and a period of 3ms [2].

4 or 16 neighboring electrodes were connected in parallel to one driver circuit. Biphasic rectangular voltage waveforms were used because they provide the highest charge injection capacity for given electrodes [2]. The voltage limits were set by an adjustable voltage limiter. After the anodic pulse there was an electrode discharge via a switch having an on-resistance value of 1kΩ. We assume that the electrode potential plays the major role in electrode lifetime [4], so the discharge current was not controlled and investigated.

During the lifetime tests, every few days the electrode voltages and currents were measured and electrode photos were made. The (anodic) charge injection capacity was calculated at each measurement via LabVIEW by integrating the anodic current pulse over time (i.e., over 0.5ms anodic pulse length). We should note that the charge injection capacity depends on the pulse lengths [3]. The calculated transferred charge was normalized to the area of the electrodes to obtain the charge injection capacity per unit area in mC/cm^2. Fig. 4 shows the current waveform and the calculated transferred charge for 16 electrodes and $\pm$2V rectangular electrode voltage in one measurement. As we see from the Figure, the transferred anodic charge is about 550nC. This corresponds to an injected charge of 1.375mC/cm^2.

We ran several experiments with different MEAs with biphasic voltage pulses of amplitudes from $\pm$0.6V to $\pm$2V. In [2] we found the potential range for reliable electrode operation in the case of TiN as electrode material. Here we tried to classify and illustrate various results via diagrams.

We measured the injected charge per unit area regularly as explained in the above example, and sketched this over time for different biphasic voltage pulse amplitudes. For every case, three experiments with three different MEAs were run. Fig. 5 shows some of our results for the different cases. Not all of the results are included here because they were more or less similar, with the absolute values of the charge injection having a variation of about 10% among the 3 experiments. The experiments did not last for the same time length. We stopped the experiment if there was no big change after a long time or there was a major drop in the transferred charge compared to the experiment beginning.

Fig. 5 shows that the case $\pm$2V connected to 16 neighboring electrodes suffers a major drop after about 30 days. The drop occurs abruptly, i.e. the transferred charge remains relatively constant for 20 days, and then it drops to almost a half within 10 days. It drops very slowly (only 16%) in the next 32 days.

Fig. 6 shows the appearance of the electrodes after the abrupt drop. The surface of the electrodes suddenly becomes dark. However, the electrodes continue to operate after this abrupt drop with the charge injection falling slowly. For $\pm$1V, the charge injection drops slowly and there is no abrupt drop. If the electrode potential remains inside the

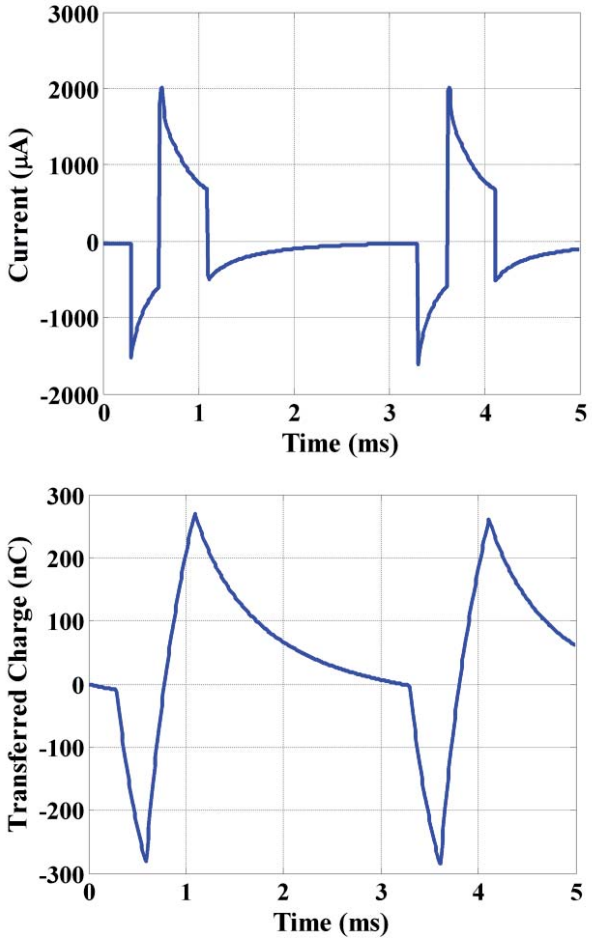

Fig. 4. Measured electrode current and calculated transferred charge of 16 electrodes for a biphasic rectangular ±2V voltage waveform.

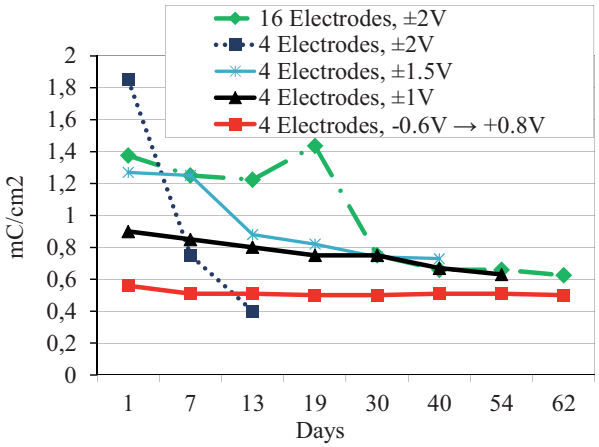

Fig. 5. Charge injection over time for different experiments.

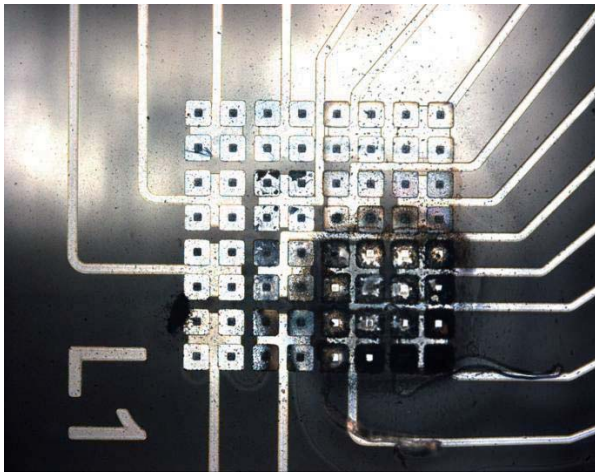

Fig. 6. Active electrode darkening effect with ±2V voltage pulses. The 16 active electrodes are on the bottom right corner. The others were not driven.

water window ($-0.6V \rightarrow 0.8V$), no charge injection drop is observed after 62 days. No optical damage was observed as well. So we confirm our previous study that for avoiding electrode damage, electrode potential must be kept inside the water window [2].

Another fact to be learned from Fig. 5 is that a lower number of active electrodes provides higher charge injection per unit area at the beginning but is more susceptible to performance deterioration. In the case of ±2V and 4 electrodes the huge drop occurs right at the beginning. Optical change was observed just 7 days after the experiment start. This may be due to the fact that when the number of active electrodes is less, the potential difference between the electrode metal and immediate surrounding solution is higher, due to the more compact overall electrical field distribution. This causes a higher voltage drop on the electrodes' Helmholtz capacitor, causing a faster deterioration. A detailed analytical study on electrical field distribution around electrodes can be found in [11].

V. CONCLUSION

We showed how adding a simple hardware to a stimulator chip could make iridium activation possible. In designs like [7], there is already a discharge transistor which could be used for electrode activation. In others a MOS transistor with a control circuit may be added. Activating iridium is a compromise: It enhances charge injection capacity but degrades mechanical properties and electrodes homogeneity [6], so iridium should not be activated if it can provide enough charge injection capacity. We investigated the lifetime of iridium electrodes with a method similar to [2]. We documented all performed measurements of charge injection versus time for different biphasic voltage pulse amplitudes. The most important graphs obtained are presented in Fig. 5.

REFERENCES

[1] Naser Pour Aryan, Christian Brendler, Viola Rieger, Steffen Kibbel, Alex Harscher, Gerhard Heusel, and Albrecht Rothermel, "A Comparison of TiN, Iridium and Iridium Oxide Stimulating Electrodes for Neural Stimulation", IASTED international conference, BioMed12, Innsbruck, Austria, February 15-17, 2012

[2] Naser Pour Aryan, Mohammad Imam Hasan Bin Asad, Christian Brendler, Steffen Kibbel, Gerhard Heusel, and Albrecht Rothermel, "In vitro Study of Titanium Nitride Electrodes for Neural Stimulation", 33rd Annual International IEEE EMBS Conference, Boston, U.S.A., August 30 - September 3 2011

[3] James D. Weiland, David J. Anderson, and Mark S. Humayun, "In Vitro Electrical Properties for Iridium Oxide Versus Titanium Nitride Stimulating Electrodes," IEEE Transactions on biomedical engineering, Vol. 49, No. 12, December 2002.
[4] Stuart F. Cogan, "Neural Stimulation and Recording Electrodes," EIC Laboratories, Inc., Norwood, Massachusetts 02062
[5] Xenia Beebe and T.L. Rose, "Charge Injection Limits of Activated Iridium Oxide Electrodes with 0.2ms Pulses in Bicarbonate Buffered Saline", 1988
[6] Wigand Poppendieck, "Untersuchungen zum Einsatz neuer Elektrodenmaterialien und deren Evaluation als Reiz- und Ableitelektrode," Dissertation, University of Saarland, 2009.
[7] Rothermel, L. Liu, N. Pour Aryan, M. Fischer, J. Wnschmann, S. Kibbel, and A. Harscher, "A CMOS Chip With Active Pixel Array and Specific Test Features for Subretinal Implantation," IEEE Journal of Solid-State Circuits, Special Issue on ISSCC 2008, vol. 44, no. 1, 2009
[8] E. Noorsal, K. Sooksood, H. Xu, R. Hornig, J. Becker and M. Ortmanns, "A Neural Stimulator Frontend with High-Voltage Compliance and Programmable Pulse Shape for Epiretinal Implants", IEEE Journal of Solid-State Circuits, San Francisco, CA USA, January 2012
[9] Kuanfu Chen, Zhi Yang, Linh Hoang, James Weiland, Mark Humayun, and Wentai Liu, "An Integrated 256-Channel Epiretinal Prosthesis", IEEE Journal of Solid-State Circuits, San Francisco, CA USA, 45(9): 1946-1956, 2010
[10] T. Tokuda et al., "CMOS based Smart-electrode-type Retinal Stimulator with Bullet-shaped bulk Pt Electrodes", 33rd Annual International IEEE EMBS Conference, Boston, U.S.A., August 30 - September 3 2011
[11] Jay T. Rubinstein et al. "Current Density Profiles of Surface Mounted and Recessed Electrodes for Neural Prostheses," IEEE Transactions on biomedical engineering, Vol. BME-34, No. 11, November 1987.
[12] Robblee, L.S.; Rose, T.L.: "Electrochemical Guidelines for Selection of Protocols and Electrode Materials for Neural Stimulation". In "Neural Prostheses" (Hrsg.: Agnew, W.F.; McCreery, D.B.), Prentice Hall, Englewood Cliffs, New Jersey, S. 25-66, 1990